

1 **Examination of the Long-term Subsurface Warming Observed at the Apollo 15 and**
2 **17 Sites Utilizing the Newly Restored Heat Flow Experiment Data from 1975 to 1977**

3

4

5 **S. Nagihara¹, W. S. Kiefer², P. T. Taylor³, D. R. Williams³ and Y. Nakamura⁴**

6 ¹Department of Geosciences, Texas Tech University, Lubbock, TX, USA.

7 ²Lunar and Planetary Institute, Universities Space Research Association, Houston, TX, USA.

8 ³Goddard Space Flight Center, Greenbelt, MD, USA.

9 ⁴Institute for Geophysics, University of Texas at Austin, Austin, TX, USA

10 Corresponding author: Seiichi Nagihara (seiichi.nagihara@ttu.edu)

11

12 **Key Points:**

- 13 • Major portions of the previously unarchived data from the Apollo Heat Flow Experiment
14 in 1975 through 1977 have been restored.
- 15 • The newly restored data better characterize the long-term subsurface warming at the Apollo
16 15 and 17 sites than previously possible.
- 17 • We suggest that solar heat intake by the regolith increased slightly at the beginning of the
18 experiment, and that resulted in the warming.
19

20 **Abstract**

21 The Apollo Heat Flow Experiment (HFE) was conducted at landing sites 15 and 17. On
22 Apollo 15, surface and subsurface temperatures were monitored from July 1971 to January 1977.
23 On Apollo 17, monitoring took place from December 1972 to September 1977. The investigators
24 involved in the HFE examined and archived only data from the time of deployment to December
25 1974. The present authors recovered and restored major portions of the previously unarchived
26 HFE data from January 1975 through September 1977. The HFE investigators noted that
27 temperature of the regolith well below **the reach of insolation cycles** (~1 m) rose gradually through
28 December 1974 at both sites. The restored data showed that the subsurface warming continued
29 until the end of observations in 1977. Simultaneously, the thermal gradient decreased, **because**
30 **the warming was more pronounced at shallower depths**. The present study has examined potential
31 causes for the warming. Recently acquired images of the Lunar Reconnaissance Orbiter Camera
32 over the two landing sites show that the regolith on the paths of the astronauts turned darker,
33 lowering the albedo. We suggest that, as a result of the astronauts' activities, solar heat intake by
34 the regolith increased slightly on average, and that resulted in the observed warming. Simple
35 analytical heat conduction models **with constant regolith thermal properties can** show that an
36 abrupt increase in surface temperature of 1.6 K to 3.5 K at the time of probe deployment best
37 duplicate the magnitude and the timing of the observed subsurface warmings at both Apollo sites.
38

39 1 Introduction

40 Conductive heat flow through the surface of a rocky planetary body such as the Earth is
41 obtained as a product of two separate measurements: thermal gradient in, and thermal conductivity
42 of, the depth interval penetrated by a probe. The primary purpose of such measurement usually is
43 to quantify the endogenic heat flow of the planetary body. Ideally, the thermal gradient and
44 thermal conductivity measurements should be made within the depth interval where temperature
45 does not fluctuate with insolation cycles. The so-called ‘thermal skin depth’ defined as the depth
46 at which amplitude of the temperature fluctuation is $1/e$ of that of the surface (e.g., Grott et al.,
47 2007; Hayne et al., 2017), is often used as a proxy to the depth limit for the reach of insolation.
48 Thermal skin depth varies among planetary bodies, depending on the thermal properties of the
49 surface material and the period of the insolation cycle.

50 The Earth’s Moon is, so far, the only extra-terrestrial body on which heat flow
51 measurements have been made successfully. On the Apollo 15 and 17 missions, heat flow probes
52 were deployed as part of the Apollo Lunar Surface Experiments Package (ALSEP). At each
53 landing site, the astronauts drilled 2 holes, roughly 10-m apart, and installed a probe in each
54 (Langseth et al., 1976). The holes were 1- and 1.4-m deep at the Apollo 15 site and 2.4-m deep at
55 the Apollo 17 site (Fig. 1). The probes monitored surface and subsurface temperature at different
56 depths for multiple years. At the Apollo 15 site, the monitoring took place from July 1971 to
57 January 1977. At the Apollo 17 site, it took place from December 1972 to the conclusion of the
58 entire ALSEP operation in September 1977 (Bates et al., 1979). These observations showed that
59 the annual, insolation-induced, thermal waves reached ~ 1.5 -m depth. Langseth et al. (1976)
60 theoretically removed the annual thermal waves from the subsurface temperature records and
61 determined the thermal gradient associated with the endogenic heat flow. The same authors also
62 estimated thermal conductivity of the regolith by modeling the downward propagation of the
63 annual thermal waves. Endogenic heat flow was then determined to be 21 mW/m^2 at Site 15 and
64 16 mW/m^2 at Site 17.

65 Marcus Langseth, the principal investigator of the heat flow experiment (HFE), determined
66 the aforementioned heat flow values at the two Apollo sites based on the observations made
67 through December 1974. It appears that he never examined the HFE data obtained from January
68 1975 to September 1977. His final report on the HFE (Langseth, 1977) only describes the data
69 obtained through December 1974. The National Space Science Data Center (NSSDC) archived
70 the HFE dataset he processed, and it also terminates in December 1974. Langseth passed away in
71 1997 without publishing any more work on the HFE data.

72 The present authors, as well as many other contemporary researchers, have searched for
73 the HFE data from January 1975 to September 1977, because there are some unanswered questions
74 about the 1971-1974 data presented in Langseth et al. (1976). For example, subsurface regolith
75 temperature gradually increased at all depths from the time shortly after the deployment to
76 December 1974 at both Apollo sites. Possible causes of this multi-year subsurface warming have
77 been debated in recent years. Proposed possibilities include a change in the thermal properties of
78 the surface regolith induced by astronaut activity, radiative heat transfer down the borestem
79 (Siegler et al., 2010), the Moon’s 18-year orbital precession, and radiation from Earth (Wieczorek
80 and Huang, 2006; Saito et al., 2007; Dombard, 2010; Laneuville and Wieczorek, 2011). We further
81 examine these possibilities in this paper.

82 For the present study, we have restored major portions of the previously unarchived 1975-
83 1977 HFE data. Using the data from the full duration of the experiment, we characterize the multi-
84 year subsurface warming and examine possible causes. It is worth noting that much of the
85 subsurface temperature data analysis performed by the original HFE investigators was not
86 presented in major scientific journals. Instead, these investigators presented their work in
87 conference proceedings and technical reports in rather fragmented fashions, as their work
88 progressed. Some of these reports are available through the *NASA Technical Reports Server*, but
89 not all. We recovered these documents in the process of restoring the 1975-1977 HFE data. For
90 that reason, the present work also reviews some of the key findings of the original investigators
91 that were not well publicized previously.

92 **2 Background on the Apollo Heat Flow Experiment**

93 At the Apollo 15 and 17 landing sites, the astronauts used a rotary-percussive drill for
94 excavating the holes for the heat flow probes. The probes were designed for 2.5-m deep holes.
95 At the Apollo 15 site, the astronauts were not able to reach that depth. For Apollo 17, the auger
96 flute had been redesigned, and was able to reach the target depth. The borestem used for drilling
97 was left in place and served as the casing for the hole. The borestem extruded above ground. The
98 astronauts slid the sensors into the borestem (Fig. 1).

99 The heat flow probes deployed at the two sites were almost identical. Each probe unit
100 consisted of two major components. The upper component consisted of a cable with 4
101 thermocouples spaced along it, and the lower component consisted of two solid rods with a total
102 of 8 platinum resistance temperature detectors (RTDs) embedded on them (Fig. 1). Each of the
103 solid rods was 0.5-m long and 2.5-cm diameter. Fiberglass-reinforced epoxy was used for the
104 material for the rods. Four RTDs were embedded on each solid rod.

105 The uppermost and the lower most RTDs of each solid rod were paired electronically as
106 part of a Wheatstone bridge. The other, inner two RTDs were also paired in the same way (Fig.
107 1). The outer pair was called the ‘gradient bridge’ and the inner pair was called the ‘ring bridge’.
108 The instrumentation circuitry was designed to determine the average temperature and the
109 temperature difference of each RTD pair. Each gradient bridge was logged with 7.25-minute
110 intervals. The ring bridges were used mainly for the in-situ thermal conductivity measurement,
111 which did not yield satisfactory results (Langseth et al., 1976; Grott et al., 2010). The ring bridge
112 RTDs were logged much less frequently than the gradient bridges. The present study focuses on
113 the measurements made with the gradient bridges. The RTDs used for the gradient bridges were
114 able to resolve temperature difference to 0.001 K in the ‘high gain’ mode with an absolute accuracy
115 of ± 0.05 K (Langseth et al., 1972b).

116 The naming scheme for the temperature sensors in Fig. 1 follows the original scheme by
117 Langseth et al. (1976). The upper and the lower gradient bridges for Probe 1 is called ‘TG11’ and
118 ‘TG12’, respectively. The corresponding gradient bridges for Probe 2 are called ‘TG21’ and
119 ‘TG22’. The upper RTD of each bridge is ‘A’ and the lower RTD is ‘B’.

120 The material used for the solid rods is more than twenty times as thermally conductive as
121 the lunar regolith in vacuum. Prior to the Apollo missions, there was a concern that the presence
122 of the high-conductivity probe would distort the temperature field of the regolith around it and
123 result in underestimation of the geothermal gradient. This phenomenon was termed ‘thermal
124 shorting’ or ‘shunting’. By carrying out laboratory experiments, Langseth et al. (1972a)

125 determined that the thermal gradient measured by the probe is 1% less than the true value due to
126 this effect.

127 For more detailed description of the HFE instrumentation, refer to Lauderdale and
128 Eichelman (1974), Langseth et al. (1976), and Langseth (1977).

129 **3 Recovery of the 1975-1977 HFE Data and Metadata**

130 The ALSEP instruments deployed at the Apollo 12, 14, 15, 16, and 17 landing sites
131 transmitted data to the Earth from 1969 to 1977. NASA's Johnson Space Center (JSC) in Houston,
132 TX was responsible for recording the raw data received from the Moon on open-reel magnetic
133 tapes. Principal investigators (PIs) of the ALSEP experiments received tape recordings of their
134 experimental data from JSC and processed them. At the conclusion of the ALSEP operation in
135 1977, only portions of the PI-processed data were archived at NSSDC (Bates et al., 1979). The
136 raw data tapes that the PIs used were never systematically archived, and most of them (including
137 the ones for the HFE) have been lost since.

138 In the early years of the ALSEP operation, NASA was preserving the tapes recorded at the
139 downlink stations of the Manned Space Flight Network for archival purpose. These tapes were
140 called 'range tapes'. In April 1973, JSC started generating data tapes specifically for archiving,
141 and they were called 'ARCSAV tapes' (Lockheed Electronics Company, 1975). The ARCSAV
142 tapes were 7-track, digital, open-reel tapes, and each contained a day's worth of raw data as
143 received from each of the Apollo stations. JSC generated 5 ARCSAV tapes for the 5 ALSEP
144 stations every day from April 1973 to February 1976. In March 1976, University of Texas at
145 Galveston (UTG) took over the work of generating archival tapes. The tapes made by UTG were
146 called 'work tapes'. They were 9-track digital tapes, and data from all the 5 ALSEP stations were
147 meshed together in them (Nakamura, 1992).

148 The range tapes and the ARCSAV tapes were never sent to NSSDC for unknown reason.
149 Most of these tapes were lost in the years following the conclusion of the Apollo program. In year
150 2010, the present authors recovered 440 ARCSAV tapes at the Washington National Records
151 Center (Nagihara et al., 2011). These tapes contained data from April through June 1975 for all
152 of the 5 ALSEP stations. This accounts for less than 10% of the ARCSAV tapes that were
153 generated during the Apollo era. The rest of the ARCSAV tapes are still missing. Digital copies
154 of the work tapes survived in their entirety, and they have been recently archived at the National
155 Space Science Data Coordinated Archive (NSSDCA), the successor to NSSDC.

156 Even though the 440 ARCSAV tapes recovered from the Washington National Records
157 Center are more than 40 years old and degraded, we were able to recover most of their contents by
158 trying multiple data-recovery service providers. Some of the files extracted from the tapes
159 included a number of bit errors. Fortunately, because the report describing the bit-level data
160 organization for these tapes survived (Lockheed Electronics Company, 1975), we were able to
161 correct many of these errors (Nagihara et al., 2017).

162 The recording on the ARCSAV tapes and work tapes consisted of data from multiple
163 experiments intermeshed. Using the bit-level data organizations for these archival tapes described
164 previously, we extracted the HFE packets from the data recorded on the tapes. For the HFE, data
165 packets on the archival tapes consisted of digital counts representative of the voltage outputs from
166 the Wheatstone bridges and the thermocouples. They needed to be processed into scientifically
167 meaningful temperature values. The reports outlining the data processing procedure for the HFE

168 have also survived (Lauderdale and Eichelman, 1974; Langseth, 1977). However, they lack
169 information on the instrument calibration. Because the RTDs of the heat flow probes needed
170 absolute accuracy of ~ 0.05 K (Langseth et al., 1972b), each probe unit was calibrated by the
171 companies that designed and fabricated them. The calibration data were not included in any of the
172 reports or research articles previously published by the original investigators. The present authors
173 conducted a search.

174 At the conclusion of the ALSEP operation, thousands of engineering reports and memos
175 generated by the companies involved in the instrument development were moved from JSC to two
176 external locations. One was the Lunar and Planetary Institute (LPI) in Houston, TX and the other
177 was the National Archives storage facility in Fort Worth, TX. We conducted an inventory of the
178 ALSEP documents kept at these two locations. In addition, we conducted a search of the
179 documents left behind by the late Marcus Langseth at his home institution of the Lamont-Doherty
180 Earth Observatory of Columbia University. Through these searches, we were able to recover the
181 documents that described the calibration test data and the data processing procedure for each of
182 the heat flow probe units (Nagihara et al., 2014; 2017).

183 In addition to these engineering reports, we recovered the ALSEP Performance Summary
184 Reports (APSRs) at LPI. These reports were weekly logs summarizing the operational status of
185 each of the ALSEP instruments from 1973 to 1977. The logs included temperature readings from
186 the deepest sensors of all the 4 heat flow probes on the Moon once a week ('TG12B', 'TG22B' in
187 Fig. 1). Though the reports rounded the temperature values to the order of 0.1 K and did not record
188 the exact time of the day of the measurements, the temperature values are useful for the periods
189 for which archival tapes are still missing (i.e., January through March 1975, July 1975 through
190 February 1976). They are also useful in checking the validity of the data we processed for the other
191 periods.

192 The APSRs also documented how the performance of the Apollo 15 heat flow probes
193 degraded in 1976. The main electronics unit for the probes began to overheat frequently in
194 February 1976, and the temperature values became erratic. From then on, the instrumentation was
195 turned off frequently for extensive cool-down periods. The instrument appeared to stabilize in the
196 late 1976, but the problem recurred in January 1977, when the instrument was commanded off
197 permanently.

198 Figure 2 summarizes the current archival status of the HFE data. As previously mentioned,
199 no ARCSAV tape has been found for January through March 1975 and July 1975 through February
200 1976. In addition, from mid-August 1976 to late April 1977, the Apollo 17 HFE data were not
201 recorded on tapes due to the fact that its data channel was used for the Lunar Seismic Profiling
202 Experiment. For those periods, only the temperature values reported weekly in the PSRs are
203 available.

204 It should be noted that Saito et al. (2007) were the first who attempted to process the HFE
205 data recorded on the work tapes for the period of March 1976 through September 1977. However,
206 these authors lacked the probe calibration data. They assumed that all the RTDs had an identical
207 characteristic. Our comparison of the temperature values obtained by Saito et al. (2007) and those
208 reported in the APSR shows discrepancy up to 0.3 K.

209 Figure 3 combines the subsurface temperature values for 1971 through 1974, archived by
210 Langseth, and those for 1975 through 1977, obtained for the present study. Here, only the values
211 for the gradient bridges (Fig. 1) are shown. Even though the gradient bridge RTDs were logged

212 every 7.25 minutes, for reasons unexplained, the original HFE investigators down-sampled the
213 RTD temperature data to 58-minute intervals for the 1971-1974 data set archived at NSSDC. The
214 1975-1977 data, restored from the ARCSAV and work tapes for the present study, contain the data
215 with the original 7.25-minute sampling intervals.

216 The temperature values for the deepest sensors ('TG12B' and 'TG22B' in Fig. 1) reported
217 in the PSRs are also shown in Fig. 3. The availability of the APSR temperature values allowed us
218 to check the temperature values of the lower gradient bridges we processed from the archival tape
219 data. Recall that the instrumentation was designed to measure the average temperature and the
220 temperature difference between the paired RTDs for each bridge. Therefore, if the temperature
221 values for the deeper RTD can be validated by those reported in the PSR, it is mostly likely that
222 the temperature values for the upper RTD of the same pair ('TG12A' and 'TG22A' in Fig. 1) are
223 also valid. For the Apollo 15 probes, the temperature values obtained from the tape data matched
224 the PSR values within 0.05K (Nagihara et al., 2017). Note that the PSR temperature values had
225 been rounded to the order of 0.1 K.

226 For the Apollo 17 probes, the two sets of temperature values (the processed tape data vs.
227 the PSR) for the deepest sensors did not match up as well as they did with the Apollo 15 probes.
228 Those processed from the tape data for the Apollo 17 probes are ~0.2 K lower than those reported
229 on the PSR. Documents we recovered at the National Archives facility in Fort Worth and Lamont-
230 Doherty Earth Observatory indicate that the Apollo 17 heat flow probes were calibrated twice in
231 1967 and 1971. However, we were able to recover only the 1967 calibration data. It is probable
232 that some electronic components for the lower bridge sections of the probes may have been
233 replaced sometime between 1967 and 1971. Therefore, for 1975 through 1977, we only show the
234 PSR temperature values for the lower bridges ('TG12' and 'TG22' in Fig. 1) of the Apollo 17
235 probes. In contrast, the upper bridge ('TG11' and 'TG21' in Fig. 1) temperature values for the
236 Apollo 17 seem more reliable, because their temperature values from the December 31, 1974,
237 processed by Langseth, and those from April 1, 1975, processed for the present study are within
238 0.05 K from one another.

239 The temperature values for the upper bridge for Apollo 15 Probe 1 (TG11A and TG11B)
240 for 1971-1974, which were processed by the original HFE investigators, show an odd behavior.
241 The temperature values for TG11A rose and fell with exactly 1-K steps for each lunar day. In
242 addition, the temperature values of TG11B rose as high as those of TG11A at noon, even though
243 the former is buried nearly 0.5 m deeper. The data from the same RTDs in 1975, which we
244 processed, do not show such oddity. We believe that the Apollo 15 TG11 data for these sensors
245 were not processed correctly for the 1971-1974 set.

246 The temperature values for the upper gradient bridge of Probe 2 ('TG21' in Fig. 1) of
247 Apollo 15 are omitted here, because the upper part the rod was above ground (Fig. 1) and was
248 heavily influenced by the insolation cycle.

249 **4 Subsurface Temperature Record for 1971 through 1977**

250 Here we interpret the subsurface temperature record for the entire duration of the HFE
251 operation. The HFE temperature record (Fig. 3) begins when the probes had just been emplaced
252 in the holes. At both sites, the deployment took place during a lunar day. Prior to deployment,
253 the probe equipment, heated by the Sun, was much hotter than the subsurface regolith. When the
254 astronauts excavated the holes, the surrounding regolith was heated by the friction of the auger

255 rotation. For these reasons, the very beginning of the subsurface temperature record shows that
256 the excess heat of the probe and the wellbore regolith gradually dissipating away. This initial
257 temperature decay took 100 to 200 days. The original HFE investigators determined the
258 equilibrium (pre-drilling) temperatures at the depths of the RTDs by theoretical extrapolation of
259 the decay trend to infinite time (Langseth et al., 1972b; 1973). Later, the same investigators
260 examined the effect of the annual insolation cycle affecting the subsurface temperature
261 measurements, but their original estimates of the equilibrium temperatures were 'largely
262 unchanged' for TG12 of Apollo 15 and all the RTDs for Apollo 17 sites (Langseth et al., 1976;
263 Langseth, 1977). Therefore, it is believed that these equilibrium temperature estimates (Table 1)
264 were used for the thermal gradient determination at each site. The small spikes observed in the
265 early part of the records are associated with the in-situ thermal conductivity measurement attempts
266 (Langseth et al., 1972b, 1973).

267 At the Apollo 15 site, the RTDs shallower than 0.5-m depth ('TG11A' and 'TG22A' in
268 Figs. 1 and 3) clearly show the influence of both the diurnal and annual insolation cycles. The
269 annual signal can be detected down to ~1-m depth ('TG12A' and 'TG22B' in Figs. 1 and 3). The
270 annual thermal wave penetrated deeper into the regolith than the diurnal wave, because of the
271 longer period of oscillation. Langseth et al. (1976) and Langseth (1977) analyzed the power
272 spectrum of the subsurface temperature records and concluded that the annual fluctuation can be
273 detected down to ~1.5-m depth (Table 1). However, in practicality, the RTDs placed deeper than
274 1-m depth (TG12B at Apollo 15 and all the RTDs at Apollo 17) do not show any obvious cyclic
275 trend, the small annual fluctuation, with amplitudes less than 0.01 K does not have significant
276 impact on the thermal gradient determination. Therefore, 1 to 1.5 m can be considered as **the depth**
277 **limit for insolation-related thermal waves.**

278 All the RTDs show gradual warming trend after the initial cool-off period of 100 to 200
279 days. For example, at the Apollo 15 site, TG12B at 1.39-m depth recorded its minimum
280 temperature value (253.0 K) roughly 100 days into deployment. Since that time, temperature
281 gradually rose to 253.7 K in December 1975, right before the instrument failure. TG12B of Apollo
282 17 at 2.34-m depth recorded its minimum temperature (256.5 K) about 200 days into deployment,
283 and it gradually warmed to 256.9 K when the experiment concluded in September 1977.

284 These subsurface warming trends below the thermal skin depth were already recognized
285 by the original HFE investigators (Langseth et al., 1976), but availability of the newly restored
286 HFE data from 1975 to 1977 enables us to characterize them in more detail. Especially for the
287 Apollo 17 site, the duration of data availability has more than doubled, because of the restoration.
288 If based on the 1972-1974 data alone, it is not clear whether or not the deepest RTDs of the Apollo
289 17 probes show any significant warming trend. Combined with the 1975-1977 data, the full record
290 clearly shows that their temperature rose.

291 At all HFE sites, the RTDs at shallower depths saw greater temperature increases. As a
292 result, the thermal gradient decreased with time. For example, for Probe 1 of the Apollo 15 site,
293 the thermal gradient based on the initial temperature decay of the lowest 2 RTDs is 1.74 K/m
294 (Langseth et al., 1972a). In June 1975, the thermal gradient of the same probe was reduced to 0.75
295 K/m.

296 **5 Potential Causes of the Multi-year Subsurface Warming**

297 It is almost certain that the multi-year subsurface warming observed at both Apollo sites
298 originated from the surface and propagated downward, rather than upward from the interior of the
299 Moon. Two lines of evidence support this. First, the shallower RTDs experienced greater
300 temperature increases. Second, the onset timing of the warming is later for the deeper RTDs. **For
301 example, temperature of the uppermost RTD (1.33-m depth) of Probe 1 of Apollo 17 started rising
302 by April of 1973 and resulted in more than 1.5-K increase, while the deepest RTD (2.33-m depth)
303 of the same probe did not start rising till mid-1974 and increased by 0.4 K.**

304 Some previous researchers, including the original HFE investigators, offered explanations
305 for the occurrence of the long-term subsurface warming. These explanations can be divided into
306 two groups. The first group (Wieczorek and Huang, 2006; Saito et al., 2007; Huang, 2008)
307 suggests that there may be fluctuations in the surface heat intake in periods longer than the annual
308 insolation cycle **and that they reach beyond 1.5-m depth**. The second group (Langseth et al., 1976;
309 Dombard, 2010) suggests that the surface thermal setting of the two Apollo sites changed abruptly
310 when the astronauts installed the probes, and that had a long-term impact on subsurface
311 temperature.

312 Resolution of this problem is crucial in two aspects. First, depending on the cause of the
313 warming, the heat flow values determined by the original investigators may need to be revised.
314 Note that the thermal gradients at these sites changed over time as a result of the long-term
315 warming. Second, instruments for future heat flow measurements on the Moon must be designed
316 to mitigate the cause of the warming. For example, **if insolation-related surface temperature
317 fluctuation can penetrate much deeper than 1.5 m**, the heat flow probes on future missions may
318 need to penetrate deeper than the Apollo probes did.

319 In this section, we test the previously proposed mechanisms that may have caused the
320 subsurface warming using the newly restored heat flow data. We also review other previous
321 researchers' arguments for and against these mechanisms. First, the original HFE investigators and
322 Dombard (2010) suggested that the activity of the astronauts altered the thermal properties of the
323 surface regolith and resulted in an increase of equilibrium surface temperature (Langseth et al.,
324 1976; Langseth, 1977). The uppermost several centimeters of the lunar regolith at the Apollo
325 landing sites consisted of loose, very fine-grained particles (e.g., Keilm et al., 1973; Carrier et al.,
326 1991). The photographs taken by the astronauts documented that they were disturbed (Fig. 4).
327 Using the 1971-1974 HFE data, Langseth (1977) constructed a thermal model in which the surface
328 area within a certain radius around the probe experienced a sudden increase in the equilibrium
329 surface temperature. **Langseth's model** showed that a 2 to 4 K increase in the surface temperature
330 can explain the observed subsurface warming at both HFE sites. The original HFE investigators
331 did not offer a specific mechanism for the surface temperature increase, however.

332 Second, Wieczorek and Huang (2006) and Saito et al. (2007) suggested that the Moon's
333 orbital precession with a period of 18.6 years might have caused a temperature oscillation of the
334 subsurface regolith well beyond the presumed skin depth. Day-time peak temperature on the lunar
335 surface varies over a year as the Sun's altitude shifts. The orbital precession modulates the annual
336 swing of the peak temperature. This can be seen on the temperature records from the
337 thermocouples that lay on/over the lunar surface at the two Apollo sites (Nagihara et al., 2010).
338 However, Laneuville and Wieczorek (2011), by carrying out numerical simulations of the heat
339 exchange at the lunar surface, showed that this modulation results in little variation in the

340 equilibrium surface temperature from one year to next year. Saito et al. (2008) suggested that,
341 because the Apollo 17 site was in a valley, lunar day length at the site was affected by the surface
342 topography, and that the combined effect of the precession and the topography might have caused
343 the average day length to gradually increase. These authors did not discuss whether or not the
344 same mechanism would apply to the Apollo 15 site.

345 Third, Huang (2008) suggested that radiation from the Earth may significantly affect the
346 night-time surface heat exchange of the nearside of the Moon. He also observed that the pre-dawn
347 surface temperature values recorded at the Apollo 15 site increased by 1 to 2 K from July 1971 to
348 December 1974, and he attributed it to a possible increase in radiation from the Earth. He further
349 argued that this period coincided with the so-called ‘Global Dimming’ episode (e.g., Stanhill and
350 Cohen, 2001), during which time, the radiation reflected by the Earth should have increased by
351 ~5%. Another study (Miyahara et al., 2008) suggests, however, that such an increase in the
352 radiation from the Earth is negligible at the mid-latitude of the Moon, where the radiation reaching
353 from the Earth has been estimated to be only 0.07 W/m².

354 Fourth, radiative heat transfer of the insolation down the borestem may have amplified the
355 thermal shorting between the surface and the subsurface (Siegler et al., 2010). As mentioned
356 previously, the RTDs placed shallower than 1-m depth detected the diurnal insolation thermal
357 wave propagating down into the regolith (Fig. 3). There should be a considerable phase lag in
358 temperature oscillation between the surface and several tens of centimeters subsurface due to the
359 low thermal conductivity (0.01 to 0.02 W/mK) of the regolith. Langseth (1977) noted in the Apollo
360 15 Probe 1 data that the phase lag between the lunar surface temperature (observed by the
361 thermocouples) and the RTD at 0.35-m depth (TG11A in Fig. 1) was shorter than expected. He
362 suggested that radiative heat transfer through the borestem may have caused it. Langseth did not
363 specifically suggest this as the cause of the subsurface warming observed.

364 **6 Discussion**

365 6.1 Photometric Changes in Surface Regolith Resulted from the Astronauts’ Activities

366 Although two of the aforementioned four mechanisms (the Moon’s orbital precession and
367 the radiation from the Earth) may have some impact on the heat balance of the lunar surface,
368 quantitative modeling (Laneuville and Wieczorek, 2011; Miyahara et al., 2008) has shown that
369 they are not likely to have resulted in a large enough increase in the surface equilibrium
370 temperature. Here, we primarily examine the other two mechanisms: the astronaut-induced
371 disturbance of the regolith and the solar radiation down the borestem.

372 The original HFE investigators (Langseth et al., 1976) did not offer a specific mechanism
373 on how the astronaut-induced disturbance of the surface regolith lead to an increase in its
374 temperature. We believe that a decrease in albedo is the most likely mechanism. The astronaut-
375 induced disturbance darkened the surface regolith and caused it on average to absorb more solar
376 heat. There is no doubt that the astronauts’ walking on the regolith altered the texture and the
377 photometric properties of its surface. Some of the photographs taken by the astronauts show that
378 the areas and the paths they walked (and drove the Lunar Roving Vehicles) turned darker overall
379 (Hapke, 1972). The images recently obtained by the Lunar Reconnaissance Orbiter Camera
380 (LROC) also show that the areas of the Apollo astronauts’ activities are darker than the
381 surrounding, undisturbed areas (Fig. 5). There is a region of regolith brightening within about 50
382 meters of the Apollo 17 Lunar Module, which is likely due to the descent engine’s exhaust plume.

383 However, the darkening of the regolith along the astronauts' tracks occur far beyond the Lunar
384 Module. So this darkening is not caused by the Lunar Module exhaust plume (Fig. 5, right).

385 It has been suggested that this darkening is primarily due to the roughening of the surface.
386 Because of their extremely angular shape, lunar regolith particles are adhesive to one another (e.g.,
387 Carrier et al., 1991). When the particles are kicked up by the astronauts' steps, they fly out in
388 small clumps, rather than as single particles (Hapke, 1972). The surface disturbed by the
389 astronauts' activities becomes cloddy and rough in mm-cm scale (Kaydash et al., 2011). The
390 individual small topographic features cast shadows around them and the surface appears darker
391 overall. Isolated footprints seem brighter than the surrounding due to the compaction and local
392 smoothing of the regolith (Fig. 4), but that also depends on the view angle. Areas of multiple,
393 overlapping footprints appear darker (Clegg et al., 2014).

394 Here, we estimate how much lowering of the albedo is necessary in increasing the lunar
395 surface temperature by 2 to 4 K, as suggested by Langseth (1977). The well-known planetary
396 radiative equilibrium temperature equation is given as (e.g., de Pater and Lissauer, 2010):

$$397 \quad T_{eq} = \left(\frac{I(1-a)}{4\varepsilon\sigma} \right)^{\frac{1}{4}}, \quad (1)$$

398 where T_{eq} is the equilibrium temperature, I is the insolation, a is the bond albedo, ε is the
399 thermal emissivity, and σ is the Boltzmann constant ($5.67 \times 10^{-8} \text{ W}/(\text{m}^2 \cdot \text{K}^4)$). The average
400 insolation for the mid-latitude of the Moon has been estimated to be $I = 662 \text{ W}/\text{m}^2$ (Miyahara et
401 al., 2008). The recent analysis of the DIVINER data suggested $\varepsilon = 0.97$ to 0.98 and $a = 0.05$ to
402 0.2 globally (Vasavada et al., 2012). Using these numbers, a 3-K increase in equilibrium
403 temperature requires less than 0.05 reduction in albedo. That is within the range of natural
404 variation of the observed albedo.

405 6.2 The Effect of Surface Warming

406 Next, using mathematical models, we examine how such an increase in the surface
407 temperature affects the subsurface temperature in the depth range of the heat flow probe
408 measurements. It should be noted that Langseth (1977) performed such an analysis, but he used
409 only the 1971-1974 HFE data, and his two-dimensional heat conduction model outcomes were
410 somewhat affected by his estimation of the radius of disturbed area, which was not well
411 constrained. Here we use the data from the full duration of the HFE (1971 to 1977), but limit the
412 model to heat conduction in the vertical direction only. As seen on the LROC images (Fig. 5), the
413 disturbed areas around the probe deployment sites are much wider than the length of the heat flow
414 probes (1.5 to 2.5-m). Therefore, the 1-D approximation should suffice.

415 Our models assume that thermal property of the regolith is constant through the depth
416 interval penetrated by each probe for simplicity. Previous studies, based on their observations of
417 the diurnal temperature swings at the surface, estimated that the uppermost 10 cm of regolith is
418 much less thermally conductive (Keihm et al., 1973; Vasavada et al., 2012; Hayne et al., 2017)
419 than at greater depths. Thermal conductivity of the uppermost regolith may also vary with
420 temperature (Cremers, 1975), increasing during the lunar day and decreasing during the night.
421 Accounting for these spatial and temporal variations would be very important if we were
422 attempting to model the surface heat exchange associated the diurnal insolation cycle. The original
423 HFE investigators found, however, that the thin low-conductivity layer at the surface made little

424 difference in their modeling of the annual thermal waves reaching much greater depths (Langseth,
 425 1977). They also found that the thermal conductivity and diffusivity of the regolith below the thin
 426 surface layer is fairly uniform (Langseth et al., 1976). Here, in modeling the multi-year warming
 427 observed at the depths beyond the reach of the insolation-induced thermal waves, we believe a 1-
 428 D models with constant thermal properties is sufficient.

429 The subsurface temperature responding to an instantaneous heating of the surface can be
 430 expressed mathematically as (e.g., Carslaw and Jaeger, 1959; Turcotte and Schubert, 1982):

$$431 \quad T(z, t) = T_1 - (T_1 - T_0) \cdot \operatorname{erfc}\left(\frac{z}{2\sqrt{\kappa t}}\right), \quad (2)$$

432 where T_0 is the original surface regolith temperature, T_1 is the new surface temperature, κ
 433 is the thermal diffusivity of the regolith, z is the depth, and t is the time elapsed since the
 434 disturbance. erfc is the complementary error function. This model ignores the surface temperature
 435 fluctuation associated with the diurnal and seasonal insolation cycles. T_0 in Eq. (2) should be
 436 regarded as the long-term average surface temperature prior to the probe deployment.

437 Figures 6 and 7 show the results of fitting the 1-D model to the probe data. It was assumed
 438 that the equilibrium subsurface temperatures estimated by the original investigators (Table 1) were
 439 the initial temperatures at these depths. Langseth (1977) yielded a range of estimates for the
 440 overall thermal diffusivity for each probe site (Table 2), based on two types of modeling. One was
 441 the downward propagation of the annual thermal wave, and the other was the sudden heating of
 442 the surface due to the astronauts' activities. For the present models, we chose a thermal diffusivity
 443 value near the middle of the range suggested by Langseth (1977) for each probe. The model
 444 outcomes were most sensitive to the magnitude of the temperature increase at the surface, $T_1 - T_0$.
 445 We used a grid search approach, varying the $T_1 - T_0$ values with 0.1-K steps and visually examined
 446 the fit. Therefore, we do not claim that these models are the most optimal statistically, but we
 447 simply suggest that they adequately demonstrate reasonable fit with the data. Figure 6 also shows
 448 how the temperature-versus-depth relationship changed over time for Probe 1 of Apollo 17. It
 449 clearly shows that thermal gradient decreased.

450 We also tested a case in which surface regolith temperature increased gradually (linearly)
 451 since the time of probe deployment. The model for gradual warming is also based on a 1-D
 452 analytical solution assuming uniform thermal diffusivity (Carslaw and Jaeger, 1959):

$$453 \quad T(z, t) = kt \left\{ \left(1 + \frac{z^2}{2\kappa t} \right) \operatorname{erfc}\left(\frac{z}{2\sqrt{\kappa t}}\right) - \frac{z}{\sqrt{\pi\kappa t}} \exp\left(-\frac{z^2}{4\kappa t}\right) \right\} \quad (3)$$

454 where k is the rate of temperature increase.

455 Figure 8 shows the model prediction with the data from Probe 1 of Apollo 15. It shows
 456 that if the surface temperature increased gradually, the warming in the subsurface is too slow in
 457 the beginning. The instantaneous surface heating model fits the data better.

458 6.3 Possibility of Solar Radiation Influx into the Borestem

459 As seen in Fig. 4, the top of the borestem was left open for both Apollo 15 probes. There
 460 is a strong possibility that solar radiation directly influenced the subsurface temperature
 461 measurements by the probes. For each probe, the RTDs were housed in two solid rods, each 0.5-

462 m long (Fig. 1). It has already been known that the upper rod of Probe 2 was directly influenced
463 by the diurnal insolation cycle, because it was placed very close to the top of the borestem. Here,
464 we focus on Probe 1. The uppermost RTD of Probe 1 (TG11A) was placed at 0.35-m below
465 surface, roughly 0.85-m below the top of the borestem.

466 As mentioned previously, the 1971-1974 HFE data archived by the original investigators
467 had problems with the temperature values for TG11 of Apollo 15 (Fig. 3). Figure 9 shows a
468 magnified view of the Apollo 15, Probe 1 subsurface temperature records for April through June
469 1975, restored for the present study. On May 25 (ordinal day 145), there was a total eclipse of the
470 Moon. During the eclipse, lunar surface temperature fell from ~350 K to ~150 K (Nagihara et al.,
471 2015). TG11A, placed at 0.35-m depth, also showed a sharp, brief, drop in temperature coincident
472 with the eclipse. This is a clear evidence that TG11A was directly affected by solar radiation. If
473 there was no radiative transfer down the borestem, temperature of TG11A should not have fallen
474 this abruptly in sync with the eclipse. Because the eclipse lasted only ~5.5 hours, the negative
475 thermal pulse resulted from it should have attenuated at shallower depths, if it propagated
476 downward solely by conduction.

477 Here we examine the analytical solution to a one-dimensional boundary value problem
478 (Carslaw and Jaeger, 1959) in which a half space has a uniform initial temperature of zero. At
479 time zero, surface temperature fell by ΔT and returns to zero at time $= t_1$. Then, temperature of the
480 half space is obtained as:

$$T(z, t) = -\Delta T \cdot \operatorname{erfc}\left(\frac{z}{2\sqrt{\kappa t}}\right) + \Delta T \cdot \operatorname{erfc}\left(\frac{z}{2\sqrt{\kappa(t-t_1)}}\right) \quad (4)$$

481
482 where ΔT is the temperature drop. Using $\Delta T = 200$ K, $\kappa = 4 \times 10^{-9}$ m²/s for the regolith in
483 the shallow depths (Langseth et al., 1976), and $t_1 = 5.5$ hours, we obtain the temperature
484 distribution shown in Fig. 10. The negative temperature pulse associated with the eclipse should
485 not have reached depths below 0.15 m, if solely based on heat conduction.

486 Therefore, the radiative heat transfer down the borestem impacted the upper rods of the
487 Apollo 15 probes during lunar days. However, it also appears that the upper rod blocked the
488 radiation from reaching deeper. That can also be inferred from the temperature record (Fig. 9).
489 TG11B and TG12A are only 8 cm apart in depth (Fig. 1), and their temperature-versus-time curves
490 overlie each other. However, the two curves (blue for TG11B and red for TG12A) behave
491 differently. The diurnal thermal wave is easily noticeable for TG11B, while it is very subtle for
492 TG12A. There is also a considerable phase lag between them. TG11B, a part of the upper rod,
493 was influenced by the insolation peeking down the borestem, while TG12A, a part of the lower
494 rod, was essentially shielded from the direct influence of the insolation. For Probe 2 of Apollo 15,
495 Langseth (1977) showed that the phase lag observed for TG22A (Fig. 1) is consistent with the
496 annual thermal wave propagating downward by conduction.

497 For Apollo 17, the astronauts installed radiation shields to the top of the borestem (Fig. 4)
498 and at ~0.3-m depth (Fig. 1). Therefore, the influence of radiation down the borestem should have
499 been minimized. The phase shifts observed for the diurnal and annual thermal waves are consistent
500 with them propagating down solely by conduction (Langseth, 1977). Therefore, if there were any
501 radiative flux that leaked through the two radiation shields, it would not have been significant.

502 7 Conclusions

503 The Apollo Heat Flow Experiment (HFE) was conducted at the Apollo 15 and 17 landing
504 sites from 1971 to 1977. The original HFE investigators left the data from 1975 to 1977
505 unarchived. The present study restored major portions of them. The restored data, combined with
506 the 1971-1974 processed by the original investigators, were used for better characterizing the
507 multi-year, gradual subsurface warming observed at both Apollo heat flow sites. The present study
508 examined four previously suggested mechanisms as potential causes for the warming: the Moon's
509 orbital precession, radiation from the Earth, albedo reduction of the surface regolith caused by the
510 astronauts' activities, and solar radiation into the borestems. The temperature-versus-time records
511 from the heat flow probes clearly indicate that the warming originated from the surface and
512 propagated downward. The shallower temperature sensors show greater magnitudes of warming,
513 and vice versa. Further, the onset timing of the warming is later for the deeper sensors. The
514 present study has found that only the albedo-reduction-induced surface warming can satisfy the
515 magnitude and the timing of the subsurface warming observed.

516 In view of planning additional heat flow measurements on future lunar-landing missions,
517 these findings, along with the other types of thermal disturbance a lunar lander may cause (Kiefer,
518 2012), should be taken into consideration for the probe deployment and measurement
519 methodologies. It is a major technological challenge to land a spacecraft and deploy a heat flow
520 probe while minimizing the resulting surface disturbance. One way to mitigate such problem may
521 be to equip the spacecraft with additional instruments (e.g., a radiometer) and monitor photometric
522 properties of the surface regolith as it lands. An alternative approach may be to robotically deploy
523 a probe quickly to the desired depth (2.5 to 3 m) and obtain thermal gradient and thermal
524 conductivity measurements, before the surface disturbance begins to affect the subsurface thermal
525 regime below the skin depth (e.g., Nagihara et al., 2014).

526 Acknowledgments

527 We thank Drs. Matthew Siegler and Matthias Grott for their constructive reviews of this
528 manuscript. The work presented here received financial support from the Lunar Advanced Science
529 and Exploration Research (LASER) and the Planetary Data Archiving, Restoration, and Tools
530 (PDART) programs of NASA's Science Mission Directorate. In recovering the original ALSEP
531 archival data tapes and related documents, we received assistance from the National Archive of
532 Fort Worth, the Washington National Records Center, and the Records Offices of the NASA
533 Headquarters, Johnson Space Center, and Goddard Space Flight Center. We also obtained
534 assistance from Ms. Rose Anne Weissel of Lamont-Doherty Earth Observatory in examining the
535 notes related to the Apollo Heat Flow Experiment left behind by Marcus Langseth. Ms. Stefanie
536 McLaughlin at Goddard Space Flight Center assisted in archiving the newly restored HFE data.

537 The newly restored HFE data from 1975-1977 used in Figure 3 are available as supporting
538 information for this article. The unprocessed HFE data recently extracted from the original ALSEP
539 data archival tapes are available from the National Space Science Data Coordinated Archive
540 (NSSDCA) (<https://nssdc.gsfc.nasa.gov/nmc/datasetDisplay.do?id=PSPG-00921> and
541 <https://nssdc.gsfc.nasa.gov/nmc/datasetDisplay.do?id=PSPG-00922>). The HFE data from 1971
542 through 1974, archived by the original investigators, have also been available through NSSDCA
543 (<https://nssdc.gsfc.nasa.gov/nmc/datasetDisplay.do?id=PSPG-00093> and
544 <https://nssdc.gsfc.nasa.gov/nmc/datasetDisplay.do?id=PSPG-00022>). Digital copies of the

545 ALSEP-related technical reports referenced by this article are now available through LPI
546 (<https://repository.hou.usra.edu/handle/20.500.11753/2>).
547

548 **References**

- 549 Bates, J. R., Lauderdale, W. W., & Kernaghan, H. (1979). ALSEP Termination Report (NASA
550 Reference Publication 1036), 165 pp. Washington, DC:
- 551 Carrier, W. D., III, Olhoeft, G. R., & Mendell, W. (1991). Physical properties of the lunar surface.
552 In G. H. Heiken, D. T. Vaniman, & B. M. French (Eds.), *Lunar Sourcebook* (pp. 475-594).
553 Cambridge: Cambridge University Press.
- 554 Carslaw, H. S., & Jaeger, J. C. (1959). *Conduction of Heat in Solids* (Second ed.), 510 pp. Oxford:
555 Oxford University Press.
- 556 Clegg, R. N., Jolliff, B. L., Robinson, M. S., Hapke, B. W., & Plescia, J. B. (2014). Effects of
557 rocket exhaust on lunar soil reflectance properties. *Icarus*, 227, 176-194.
558 <http://www.sciencedirect.com/science/article/pii/S001910351300393X>
- 559 Cremers, C. J. (1975). Thermophysical properties of Apollo 14 fines. *J. Geophys. Res.*, 80(32),
560 4466-4470. <https://agupubs.onlinelibrary.wiley.com/doi/abs/10.1029/JB080i032p04466>
- 561 de Pater, I., & Lissauer, J. J. (2010). *Planetary Sciences* (2nd ed.), 647 pp. New York: Cambridge
562 University Press.
- 563 Dombard, A. J. (2010). Mitigation Strategies for Astronaut Surface Disturbances During
564 Deployment of Lunar Heat Flow Experiments. Paper presented at the Ground-Based
565 Geophysics on the Moon, Houston.
566 <http://www.lpi.usra.edu/meetings/lunargeo2010/pdf/3015.pdf>
- 567 Grott, M., Helbert, J., & Nadalini, R. (2007). Thermal structure of Martian soil and the
568 measurability of the planetary heat flow. *Journal of Geophysical Research: Planets*,
569 112(E9). <https://agupubs.onlinelibrary.wiley.com/doi/abs/10.1029/2007JE002905>
- 570 Grott, M., Knollenberg, J., & Krause, C. (2010). Apollo lunar heat flow experiment revisited: A
571 critical reassessment of the in situ thermal conductivity determination. *Journal of*
572 *Geophysical Research: Planets*, 115(E11), E11005.
573 <http://dx.doi.org/10.1029/2010JE003612>
- 574 Hayne, P. O., Bandfield, J. L., Siegler, M. A., Vasavada, A. R., Ghent, R. R., Williams, J.-P., et
575 al. (2017). Global Regolith Thermophysical Properties of the Moon From the Diviner
576 Lunar Radiometer Experiment. *Journal of Geophysical Research: Planets*, 122(12), 2371-
577 2400. <http://dx.doi.org/10.1002/2017JE005387>
- 578 Hapke, B. W. (1972). The lunar disturbance effect. *The Moon*, 3(4), 456-460.
579 <https://doi.org/10.1007/BF00562465>
- 580 Huang, S. (2008). Surface temperatures at the nearside of the Moon as a record of the radiation
581 budget of Earth's climate system. *Advances in Space Research*, 41(11), 1853-1860.
582 <http://www.sciencedirect.com/science/article/pii/S0273117707004553>
- 583 Kaydash, V., Shkuratov, Y., Korokhin, V., & Videen, G. (2011). Photometric anomalies in the
584 Apollo landing sites as seen from the Lunar Reconnaissance Orbiter. *Icarus*, 211(1), 89-
585 96. <http://www.sciencedirect.com/science/article/pii/S0019103510003404>
- 586 Keihm, S. J., Peters, K., Langseth, M. G., & Chute, J. L. (1973). Apollo 15 measurement of lunar
587 surface brightness temperatures thermal conductivity of the upper 1 1/2 meters of regolith.
588 *Earth and Planetary Science Letters*, 19(3), 337-351.
589 <http://www.sciencedirect.com/science/article/pii/0012821X73900848>

590 Kiefer, W. S. (2012). Lunar heat flow experiments: Science objectives and a strategy for
591 minimizing the effects of lander-induced perturbations. *Planetary and Space Science*,
592 60(1), 155-165. <http://www.sciencedirect.com/science/article/pii/S0032063311002376>

593 Langseth, M. G., Jr. (1977). Lunar Heat-flow Experiment: Final Technical Report, 289 pp,
594 Lamont-Doherty Geological Observatory, Palisades, NY.

595 Langseth, M. G., Clark, S. P., Chute, J. L., Keihm, S. J., & Wechsler, A. E. (1972a). The Apollo
596 15 lunar heat-flow measurement. *The Moon*, 4(3), 390-410.
597 <http://dx.doi.org/10.1007/BF00562006>

598 Langseth, M. G., Jr., Clarke, S. P., Chute, J. L., Jr., Keihm, S. J., & Wechsler, A. E. (1972b). Heat-
599 flow experiment. In *Apollo 15 Preliminary Science Report (Section 11, 1-23)*. Washington,
600 D.C.: National Aeronautics and Space Administration, SP-289.

601 Langseth, M. G., Jr., Keihm, S. J., & Chute, J. L., Jr. (1973). Heat flow experiment. In *Apollo 17*
602 *Preliminary Science Report (Section 9, 1-24)*. Washington: National Aeronautics and
603 Space Administration, SP-330.

604 Langseth, M. G., Keihm, S. J., & Peters, K. (1976). Revised lunar heat-flow values. *Proc. Lunar*
605 *Sci. Conf.*, 7, 3143-3171.

606 Laneuville, M., & Wieczorek, M. A. (2011). The Heat Flow of the Moon: Influence of Long Term
607 Orbital Signals. Paper presented at the 42nd Lunar and Planetary Science Conference,
608 Houston. <http://www.lpi.usra.edu/meetings/lpsc2011/pdf/2296.pdf>

609 Lauderdale, W. W., & Eichelman, W. F. (1974). *Apollo Scientific Experiments Data Handbook*
610 (NASA TM X-58131), 1011 pp, Johnson Space Center, Houston.

611 Lockheed Electronic Company (1975). *Apollo Lunar Surface Experiment Package Archive Tape*
612 *Description Document*, 319 pp, Johnson Space Center, JSC-09652, Houston, TX.

613 Miyahara, H., Wen, G., Cahlan, R. F., & Ohmura, A. (2008). Deriving historical total solar
614 irradiance from lunar borehole temperatures. *Geophysical Research Letters*, 35, L02716,
615 doi:10.1029/2007GL032171.

616 Nagihara, S., Nakamura, Y., Kiefer, W. S., Hager, M. A., Williams, D. R., Taylor, P. T., et al.
617 (2014). Recovery of ALSEP Raw Instrument Data and Metadata. Paper presented at the
618 45th Lunar and Planetary Science Conference, Houston.
619 <http://www.lpi.usra.edu/meetings/lpsc2014/pdf/1153.pdf>

620 Nagihara, S., Nakamura, Y., Lewis, L. R., Williams, D. R., Taylor, P. T., Grayzeck, E. J., et al.
621 (2011). Search and Recovery Efforts for the ALSEP Data Tapes. Paper presented at the
622 42nd Lunar and Planetary Science Conference, Houston.
623 <http://www.lpi.usra.edu/meetings/lpsc2011/pdf/1103.pdf>

624 Nagihara, S., Nakamura, Y., Taylor, P. T., & Williams, D. R. (2015). Restoration of 1975 Apollo
625 Heat Flow Experiment Thermocouple Data from the Original ALSEP Archival Tapes.
626 Paper presented at the Lunar Exploration Analysis Group, Houston.
627 <http://www.lpi.usra.edu/meetings/leag2015/pdf/2019.pdf>

628 Nagihara, S., Nakamura, Y., Williams, D. R., Taylor, P. T., McLaughlin, S. A., Hills, H. K., et al.
629 (2017). Recent Achievement by the SSERVI ALSEP Data Recovery Focus Group. Paper
630 presented at the Annual Meeting of the Lunar Exploration Analysis Group, Houston.
631 <http://www.lpi.usra.edu/meetings/leag2017/pdf/5017.pdf>

632 Nagihara, S., Saito, Y., & Taylor, P. T. (2010). Reexamination of the Apollo 15 Heat Flow Data
633 Toward Understanding Potential Causes of the Long-Term Subsurface Warming
634 Observed. Paper presented at the 41st Lunar and Planetary Science Conference, Houston.
635 <http://www.lpi.usra.edu/meetings/lpsc2010/pdf/1353.pdf>

636 Nakamura, Y. (1992). Catalog of lunar seismic data from the Apollo Passive Seismic Experiment
637 on 8-mm video cassette (Exabyte) tapes. University of Texas Institute for Geophysics
638 Technical Report 118, 67 pp, Austin.

639 Saito, Y., Tanaka, S. T., Horai, K., & Hagermann, A. (2008). The Long Term Temperature
640 Variation in the Lunar Subsurface. Paper presented at the 39th Lunar and Planetary Science
641 Conference, Houston. <http://www.lpi.usra.edu/meetings/lpsc2008/pdf/1663.pdf>

642 Saito, Y., Tanaka, S., Takita, J., Horai, K., & Hagermann, A. (2007). Unprocessed Apollo heat
643 flow measurement data (in Japanese). *Bulletin of the Japanese Society for Planetary
644 Sciences*, 16(2), 158-164.

645 Siegler, M. A., Paige, D. A., Keihm, S. J., Vasavada, A. R., Ghent, R. R., Bandfield, J. L., &
646 Snook, K. J. (2010). Apollo Lunar Heat Flow Experiments and the LRO Diviner
647 Radiometer. Paper presented at the 41st Lunar and Planetary Science Conference, Houston.
648 <http://www.lpi.usra.edu/meetings/lpsc2010/pdf/2650.pdf>

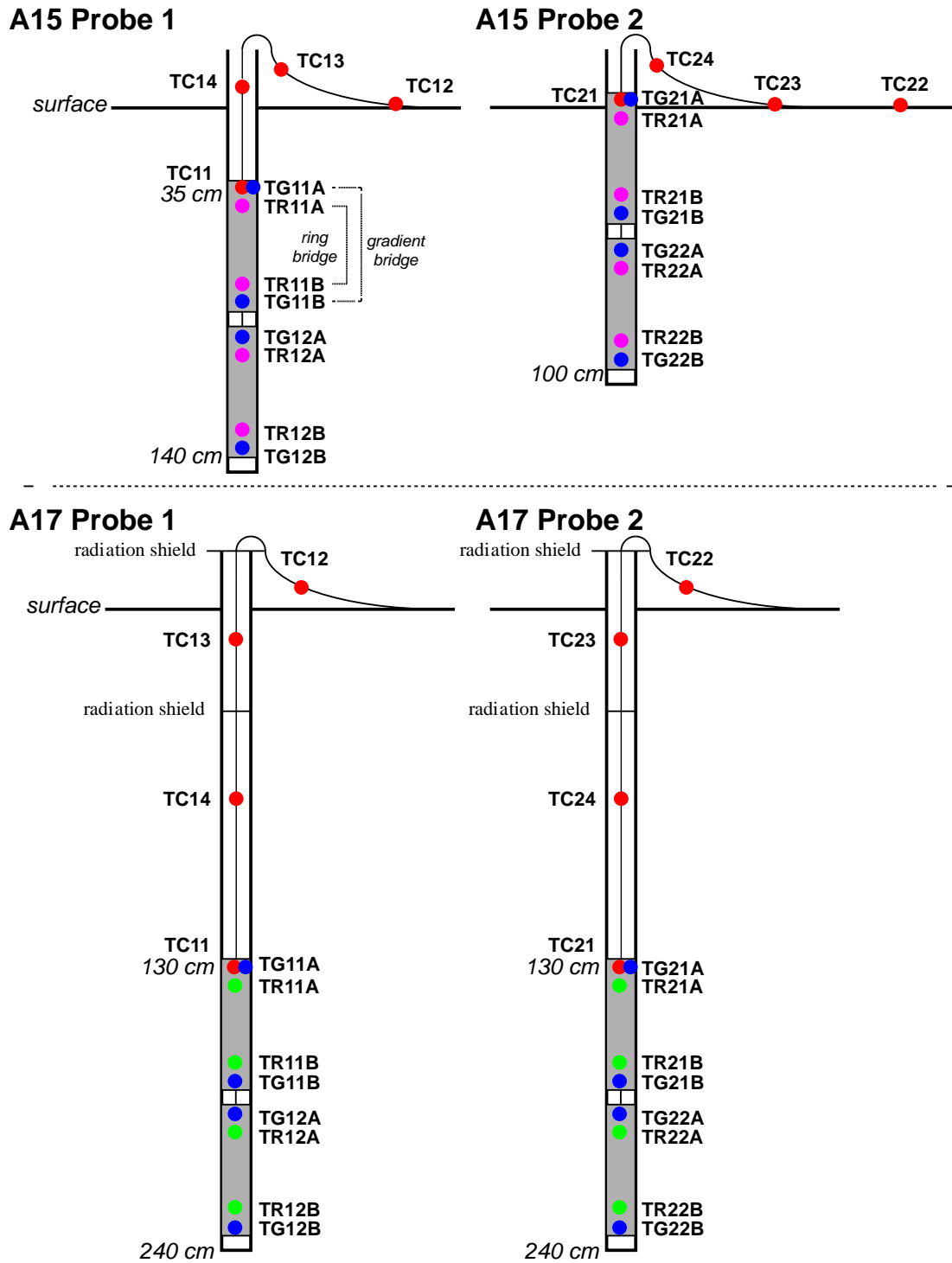
649 Stanhill, G., & Cohen, S. (2001). Global dimming: a review of the evidence for a widespread and
650 significant reduction in global radiation with discussion of its probable causes and possible
651 agricultural consequences. *Agricultural and Forest Meteorology*, 107(4), 255-278.
652 <http://www.sciencedirect.com/science/article/pii/S0168192300002410>

653 Turcotte, D. L., & Schubert, G. (1982). *Geodynamics*: 450 pp., John Wiley & Sons, New York.

654 Vasavada, A. R., Bandfield, J. L., Greenhagen, B. T., Hayne, P. O., Siegler, M. A., Williams, J.-
655 P., & Paige, D. A. (2012). Lunar equatorial surface temperatures and regolith properties
656 from the Diviner Lunar Radiometer Experiment. *Journal of Geophysical Research: Planets*,
657 117(E12), E00H18. <http://dx.doi.org/10.1029/2011JE003987>

658 Wieczorek, M. A., & Huang, S. (2006). A Reanalysis of Apollo 15 and 17 Surface and Subsurface
659 Temperature Series. Paper presented at the 37th Lunar and Planetary Science Conference,
660 Houston. <http://www.lpi.usra.edu/meetings/lpsc2006/pdf/1682.pdf>

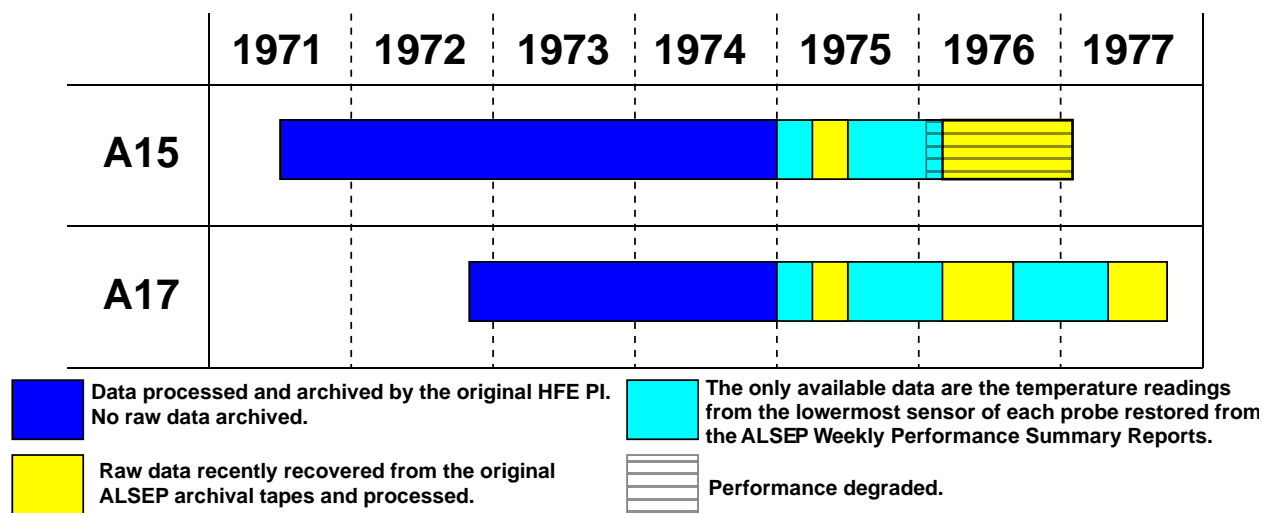
661



662

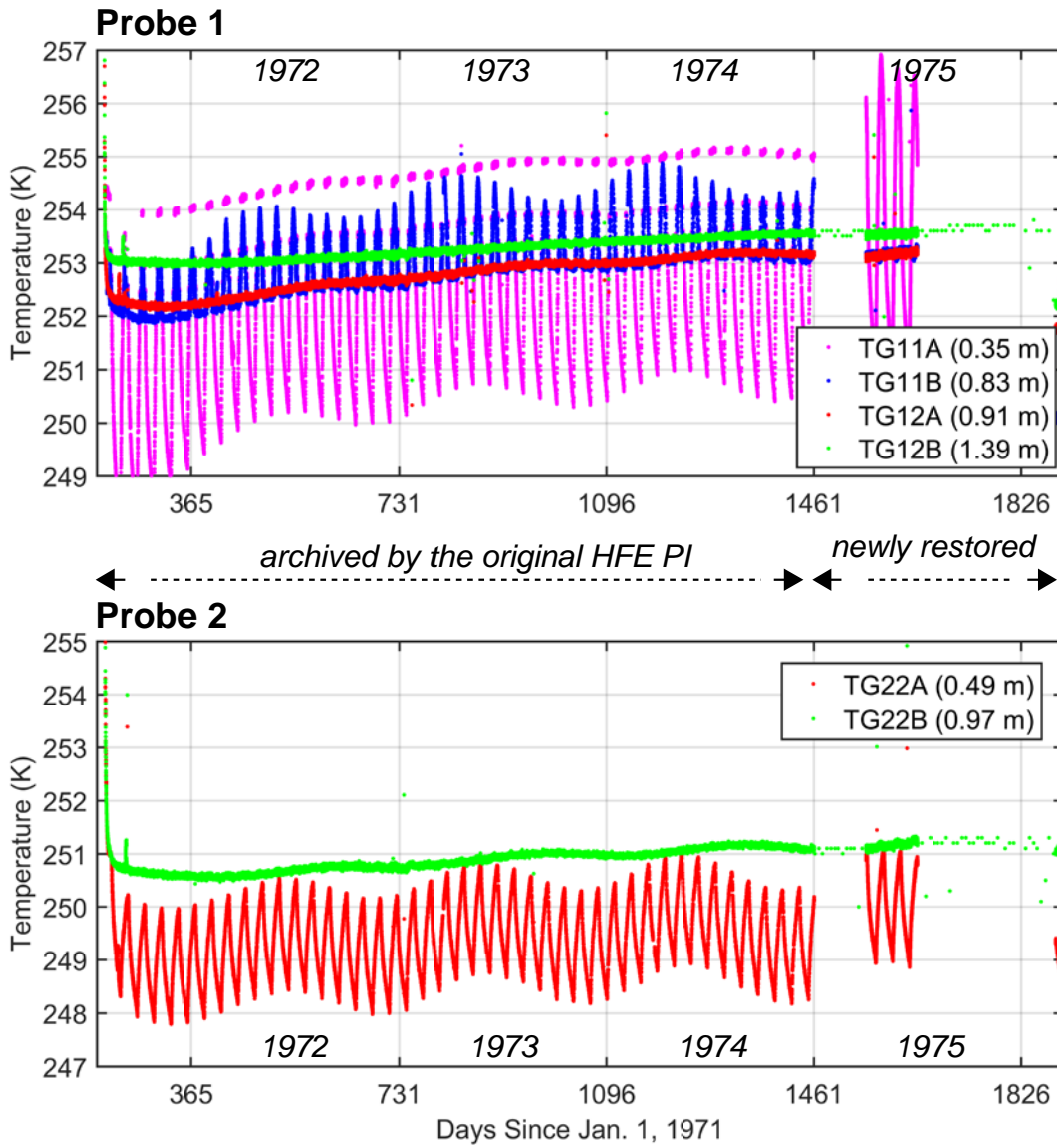
663 **Figure 1.** Schematic drawings describing the emplacement of the heat flow probes at the Apollo
 664 15 and 17 landing sites. The temperature sensors are labeled. The red dots indicate the
 665 thermocouples. The blue dots indicate the gradient bridge RTDs. The green dots indicate the ring
 666 bridge RTDs. The probe hardware was almost identical between the two landing sites except that
 667 the Apollo 17 probes were equipped with radiation shields.
 668

Archival Status of the Apollo 15 and 17 HFE Data



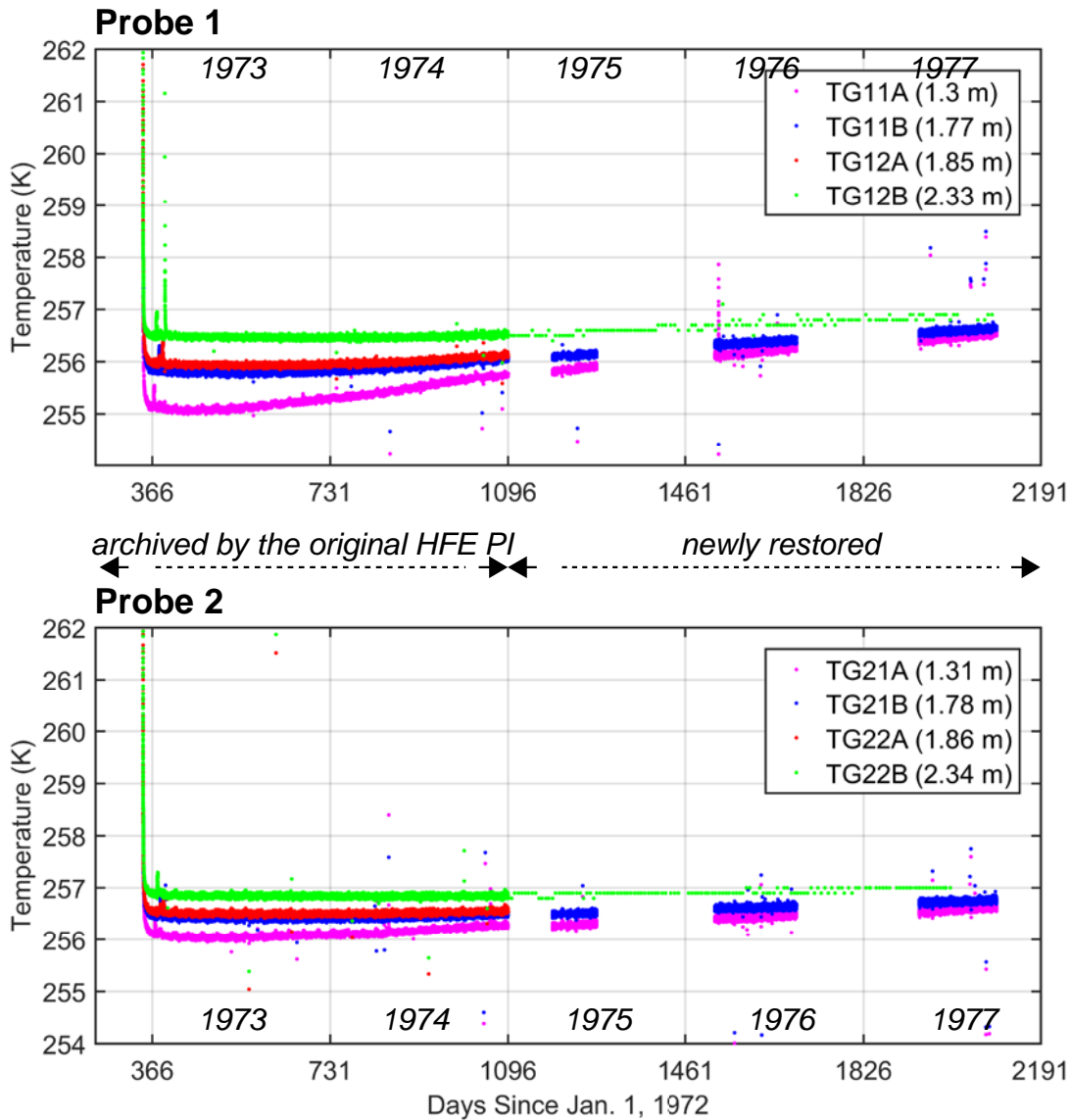
669
670
671
672
673

Figure 2. The current data archival status of the Apollo 15 and 17 Heat Flow Experiments.



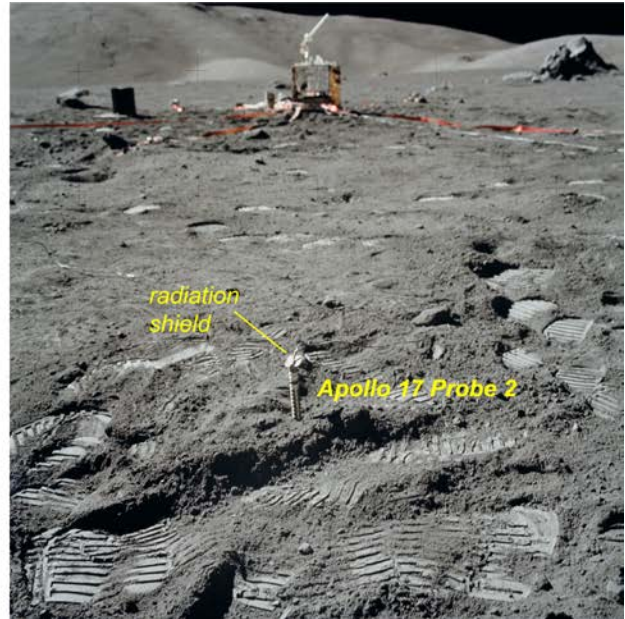
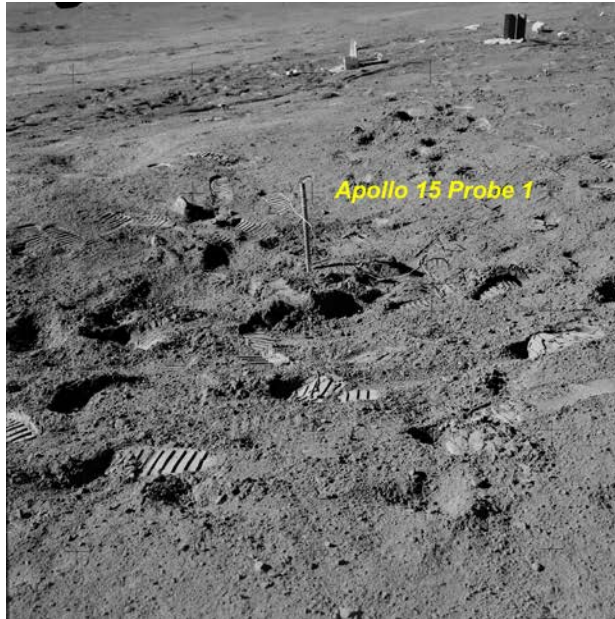
674
 675 **Figure 3a.** Temperature versus time records for the gradient bridge RTDs of the Apollo 15 heat
 676 flow probes. **The probes started operating on July 31, 1971.** The data from 1971 through 1974
 677 were processed by the original HFE investigators (Langseth et al., 1976). The data from 1975
 678 through 1977 were restored by the present authors. Refer to Fig. 1 for the positions of the
 679 individual RTDs.

680
 681



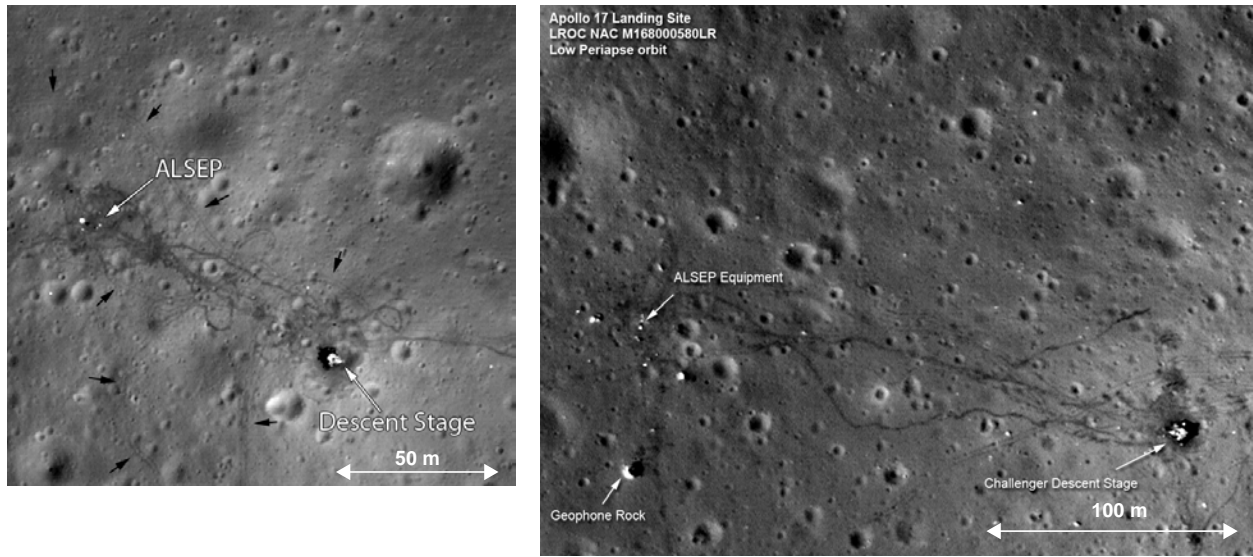
682
 683 **Figure 3b.** Temperature versus time records for the gradient bridge RTDs of the Apollo 17 heat
 684 flow probes. The probes started operating on December 12, 1972. The data from 1972 through
 685 1974 were processed by the original HFE investigators (Langseth et al., 1976). The data from 1975
 686 through 1977 were restored by the present authors. Refer to Fig. 1 for the positions of the
 687 individual RTDs.

688
 689



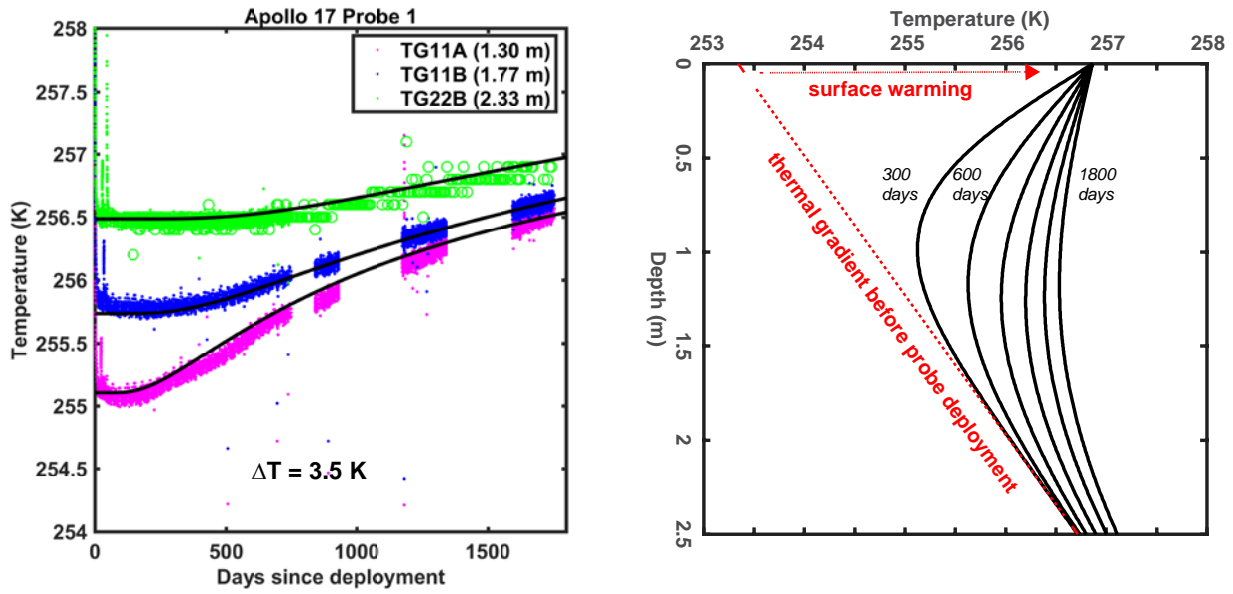
690
691
692
693
694
695
696
697
698
699
700

Figure 4. Left: Photograph by astronaut James Irwin showing the borestem and the cable of the Apollo 15 Probe 1 protruded from the ground. Around the borestem, footprints of the astronauts can be seen. Note that the top of the borestem is left open. The original photo was obtained from NASA, <https://www.hq.nasa.gov/alsj/a15/AS15-92-12406HR.jpg>. Right: Photograph by astronaut Harrison Schmidt showing the borestem and the cable of the Apollo 17 Probe 2 protruded from the ground. Note the radiation shield attached to the top of the borestem. The original photo was obtained from NASA, <https://www.hq.nasa.gov/alsj/a17/AS17-134-20493HR.jpg>.



701
702
703
704
705
706
707
708
709
710

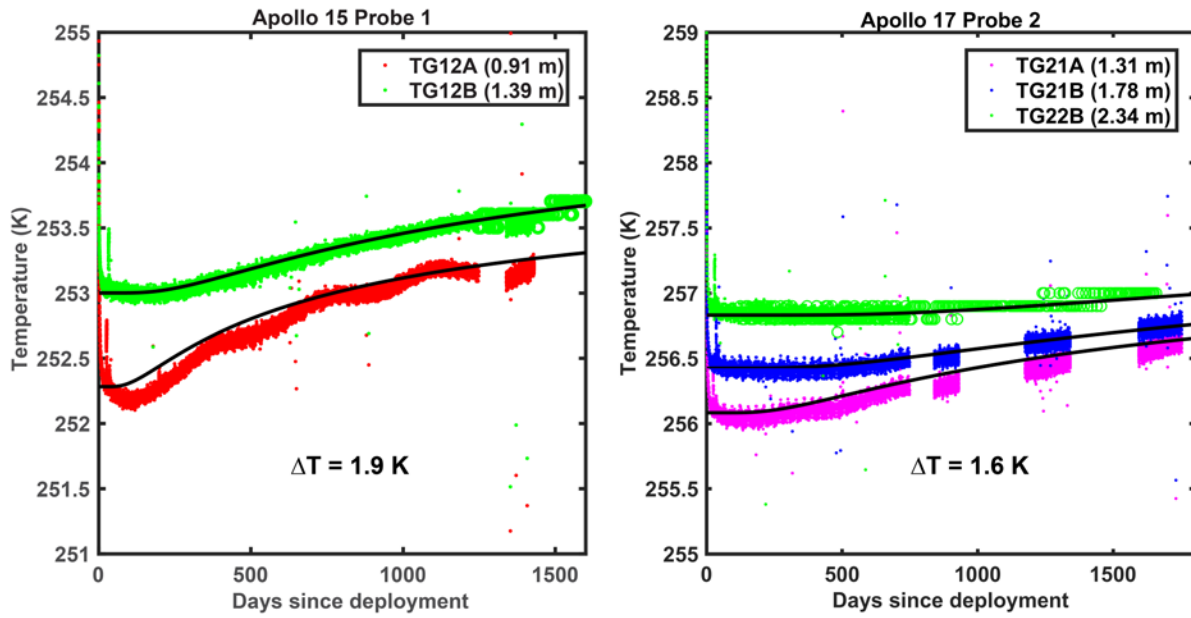
Figure 5. Left: Lunar Reconnaissance Orbiter Camera (LROC) image of the vicinity of the Apollo 15 landing site. Note that the surface around the ALSEP deployment site is darker than the surroundings. The original image obtained from NASA, https://lunarscience.nasa.gov/wp-content/uploads/2012/03/M175252641LR_ap15.png. Right: LROC image of the vicinity of the Apollo 17 landing site. Note that the surface around the ALSEP deployment site is darker than the surroundings. The original image obtained from NASA, https://www.nasa.gov/sites/default/files/images/584392main_M168000580LR_ap17_area.jpg.



711

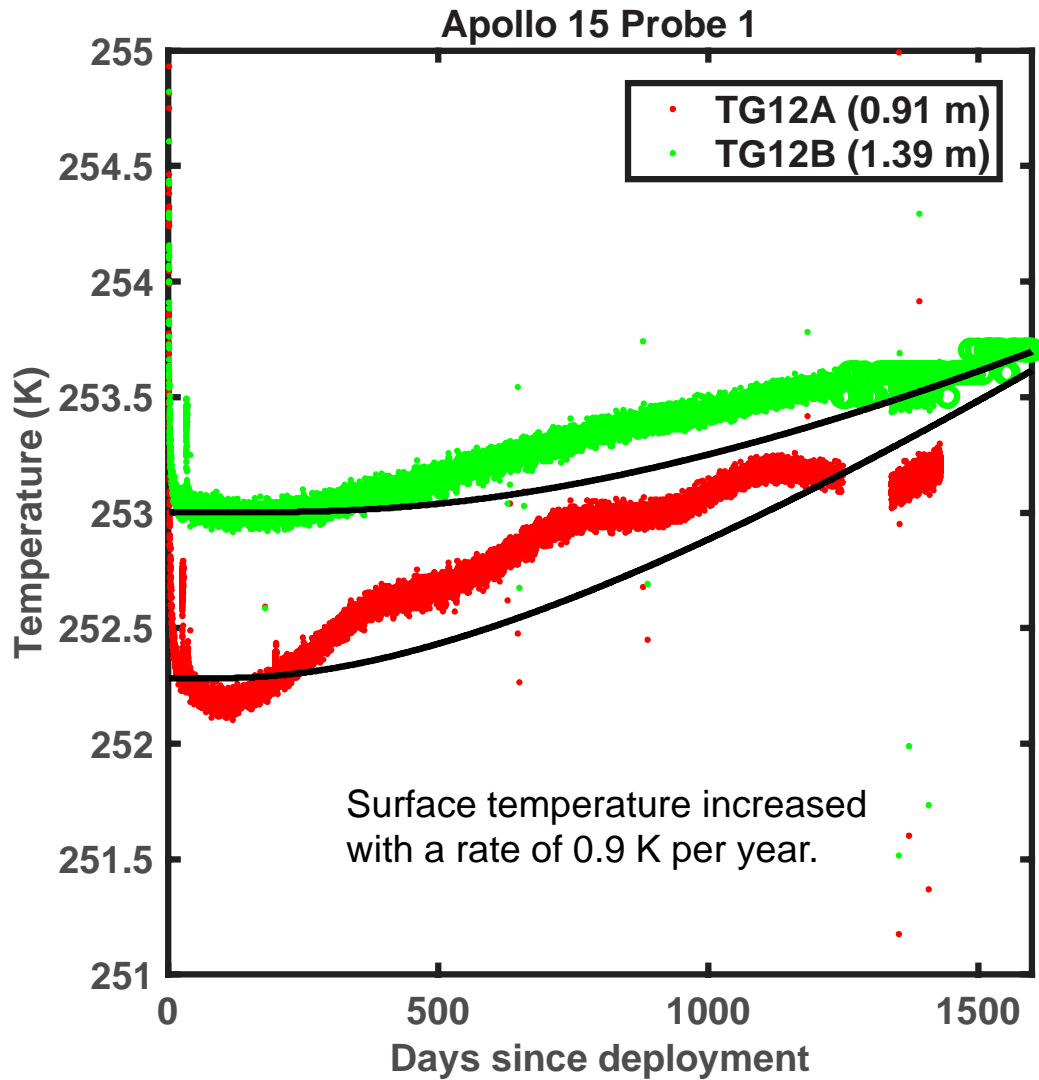
712 **Figure 6.** Left: A graph showing temperature-versus-time curves for RTDs TG11A, TG11B, and
 713 TG22B of Probe 1 of Apollo 17, predicted by the mathematical model of a sudden temperature
 714 increase at the surface at the time of probe deployment. The colored dots show the actual
 715 temperatures obtained by the same RTDs. Right: A graph showing how temperature-versus-depth
 716 relationship changed over the same time duration of the model.

717



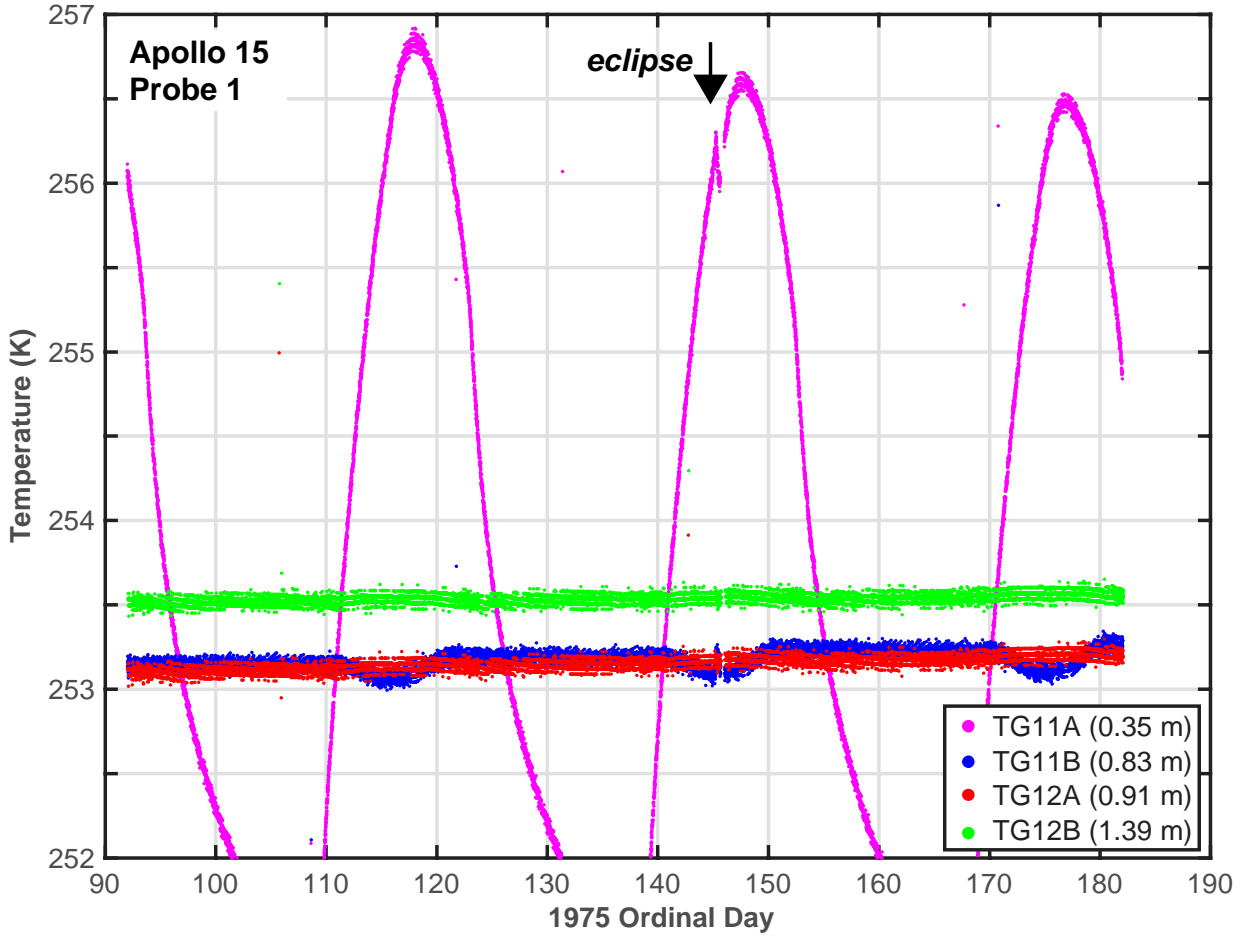
718
 719
 720
 721
 722
 723
 724

Figure 7. Temperature-versus-time curves for the RTDs of Probe 1, Apollo 15 (left) and those of Probe 2, Apollo 17 (right), predicted by the mathematical model of a sudden temperature increase at the surface at the time of probe deployment. The colored dots show the actual temperatures obtained by the same RTDs.



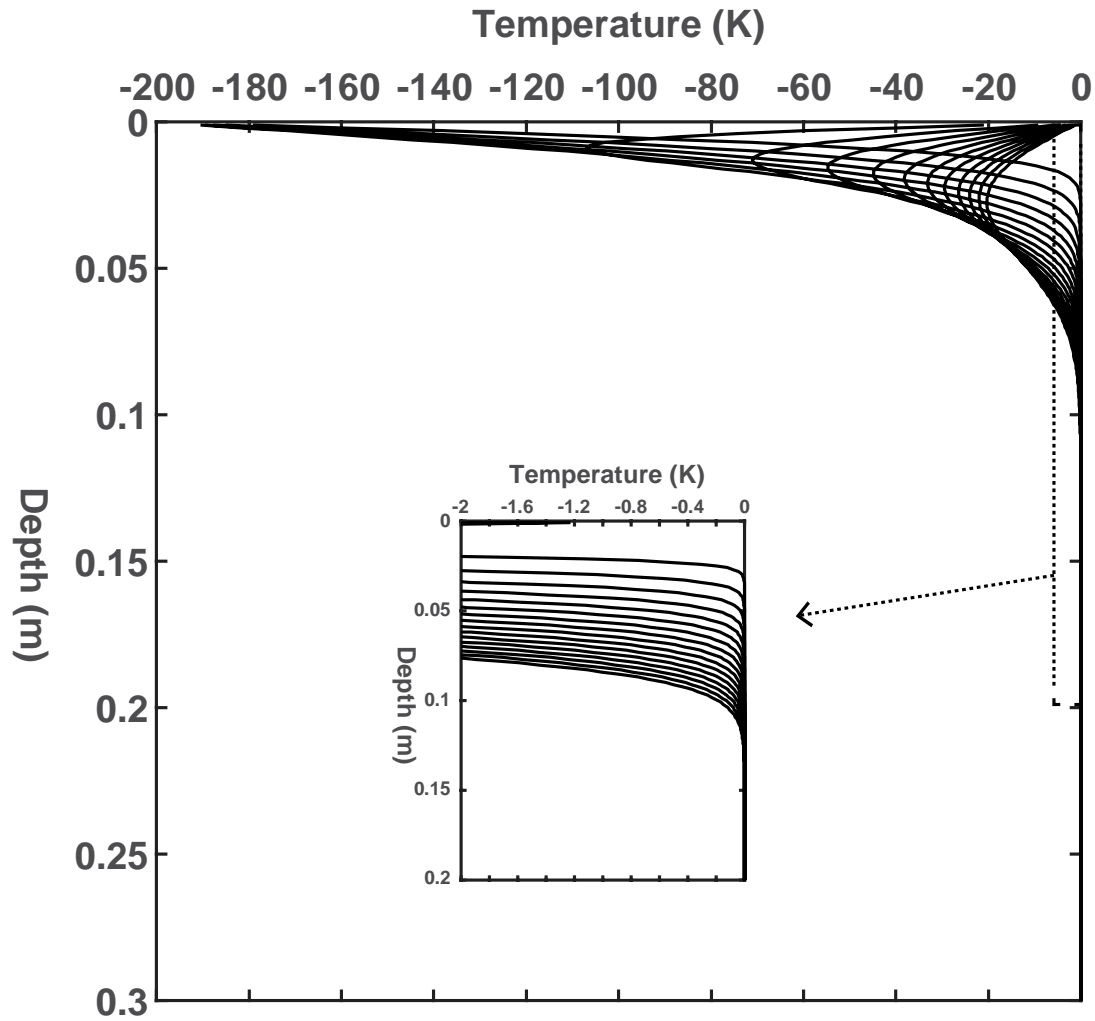
725
 726
 727
 728
 729
 730
 731
 732

Figure 8. Temperature-versus-time curves for the RTDs of Probe 1, Apollo 15 predicted by the mathematical model of a linear temperature increase at the surface since the time of probe deployment with a rate of 0.9 K per year. The colored dots show the actual temperatures obtained by the same RTDs.



733
 734
 735
 736
 737

Figure 9. A magnified view of the temperature versus time records for the RTDs of Probe 1, Apollo 15 for the period of April through June 1975, restored for the present study.



738
 739 **Figure 10.** Temperature versus depth curves obtained from the mathematical model showing how
 740 a negative temperature drop by 200 K at the surface for 5.5 hours propagates into the subsurface.
 741 The curves are drawn with 1-hour time steps. The inset shows the magnified view of the same
 742 graph for a temperature range of -2 to 0 K.
 743

744 **Table 1.** Equilibrium subsurface temperature values determined by the original HFE investigators.

Site	Probe#	Sensor	Depth (m)	Equilibrium Temperature (K)	Annual Fluctuation Amplitude (K)
Apollo 15	1	TG11A	0.35	---	0.29 ^D
	1	TG11B	0.83	251.96 ^A	0.058 ^D
	1	TG12A	0.91	252.20 ^C (252.28 ^A)	0.038 ^D
	1	TG12B	1.39	253.00 ^{A,C}	< 0.01 ^D
	2	TG22A	0.49	---	0.305 ^D
	2	TG22B	0.97	250.70 ^A	0.056 ^D
Apollo 17	1	TG11A	1.3	255.06 ^{B,C}	0.021 ^D
	1	TG11B	1.77	255.76 ^{B,C}	---
	1	TG12A	1.85	255.91 ^{B,C}	0.0038 ^D
	1	TG12B	2.33	256.44 ^{B,C}	---
	2	TG21A	1.31	256.07 ^{B,C}	0.016 ^D
	2	TG21B	1.78	256.44 ^{B,C}	---
	2	TG22A	1.86	256.48 ^{B,C}	0.0022 ^D
	2	TG22B	2.34	256.82 ^{B,C}	---

745 Data Sources: A: Langseth et al. (1972b), B: Langseth et al. (1973), C: Lauderdale and Eichelman
 746 (1974), D: Langseth (1977)

747

748 **Table 2.** A summary of the surface temperature increase estimates based on the 1-D heat
 749 conduction model of the instantaneous heating of the surface.

Probe	Surface Temperature Increase ($T_1 - T_0$) (K)	Thermal Diffusivity (m^2/s)	Thermal Diffusivity by Langseth (1977) (m^2/s)
A15 Probe 1	1.9	8.0×10^{-9}	6.0×10^{-9} to 1×10^{-8}
A17 Probe 1	3.5	8.0×10^{-9}	6.5×10^{-9} to 9.5×10^{-9}
A17 Probe 2	1.6	6.5×10^{-9}	5.5×10^{-9} to 7.0×10^{-9}

750